Turkish Journal of Electrical Engineering & Computer Sciences

http://journals.tubitak.gov.tr/elektrik/

Research Article

Turk J Elec Eng & Comp Sci
(2019) 27: 819 – 831
© TÜBİTAK
doi:10.3906/elk-1711-183

A novel design of an electromagnetically levitated vibrational viscometer for biomedical and clinical applications

Ali AKPEK*
Department of Bioengineering, Faculty of Engineering, Gebze Technical University, Kocaeli, Turkey

Received: 16.11.2017 • **Accepted/Published Online:** 29.11.2018 • **Final Version:** 22.03.2019

Abstract: Accurate determination of the viscosity behavior of fluids is extremely important, especially for biomedical and clinical applications. For example, blood viscosity is used to detect cardiovascular diseases in patients. Like blood, all body fluids and biochemical solvents used in biomedical studies are very limited resources. Therefore, a viscometer that is especially focused for biomedical and clinical applications should have the ability to obtain viscosity results from a reservoir as small as possible, in a range as wide as possible and in a period of time as short as possible. The measurements must be accurate even when the fluid temperatures shift swiftly and the test fluids pass throughout the viscometer continuously. Thus, it would be a huge advantage if a viscometer had the capability to measure simultaneously dynamic viscosity, kinematic viscosity, static viscosity, and density. However, there is no viscometer in the world that can achieve these goals. In this study, a novel electromagnetically levitated vibrational viscometer is designed to solve this problem.

Key words: Viscosity measurement, heat and mass transfer, biomedical instrumentation

1. Introduction

In both industry and academic research, the ability to gather data on the viscosity behavior of materials is extremely important. This need is especially stronger in biomedical and clinical applications. For example, blood viscosity has been used to comprehend cardiovascular diseases in medicine [1–3]. However, the viscosity of blood changes due to several parameters such as flow rate, vein type, body temperature, and even hour of the day [4–6]. Therefore, accurate data may have vital importance. In addition, since blood is a limited source, it is a necessity to obtain viscosity results from a reservoir as small as possible. Furthermore, blood viscosity is primarily required during surgical operations [7,8], and it is important to obtain viscosity values in a range as wide as possible and also in a period of time as short as possible. This is primarily similar in other types of body fluids such as urine, cerebrospinal fluid, pleural fluid, peritoneal fluid, pericardial fluid, synovial fluid, and even semen [9–11]. Similarly, the same type of problem needs to be solved in biomedical studies. Biochemical solvents that may be used in blood or other types of body fluids are also limited sources. Therefore, a viscometer that is especially focused for biomedical and clinical applications should have the ability to obtain viscosity results from a reservoir as small as possible, in a range as wide as possible, and in a period of time as short as possible even though the environmental temperatures suddenly vary. There is no viscometer in the world that could ever succeed in that until the electromagnetically levitated vibrational (ELV) viscometer. It is also not possible to measure viscosity accurately for any of the conventional viscometers while the fluid passes throughout the

*Correspondence: aliakpek@gtu.edu.tr

This work is licensed under a Creative Commons Attribution 4.0 International License.

experimental cup continuously. We can proudly say that after this study there is a viscometer that can achieve this goal. In addition, none of the current viscometers can measure dynamic viscosity, kinematic viscosity, static viscosity, and density simultaneously but the ELV viscometer can, which is another innovation. The overall comparison between the ELV viscometer and other, conventional viscometers is presented in the Table.

In the present study, the effects of nonuniform temperature fields were first investigated in detail to prove that even in very small volumes severe viscosity variations may occur as the fluid temperatures change swiftly. This is a very serious problem that needs to be solved by industry and academia to enhance fluid quality. The errors in viscosity measurements were obtained and recorded.

Table. Comparison of the ELV viscometer and other, conventional viscometers.

Viscometer Models	Dynamic viscosity (μ)	Kinematic viscosity (ν)	Static viscosity (μ x ρ)	Density (ρ)	Capability of viscosity measurement during sudden temperature variations	Capability of viscosity measurement during fluid flow
U-tube Viscometers[12, 13]	X	✓	X	X	X	X
Falling Sphere Viscometers [14, 15]	X	✓	X	X	X	X
Falling Ball Viscometers [16, 17]	✓	X	X	X	X	X
Oscillating Piston Viscometer [18]	✓	X	X	X	✓	X
Vibrational Viscometers [19, 20]	X	X	✓	X	✓	X
Quartz Viscometer [21]	X	X	✓	X	✓	X
Rotational Viscometers [22, 23]	✓	X	X	X	✓	X
Electromagnetically Spinning Sphere Viscometer [24]	✓	X	X	X	✓	X
Stabbinger Viscometer [25]	✓	✓	✓	✓	X	X
Bubble Viscometer [26]	X	✓	X	X	X	X
Rectangular Slit Viscometer [27, 28]	✓	X	X	X	X	X
Electromagnetically Levitated Vibrational Viscometer	✓	✓	✓	✓	✓	✓

Then the same experiment was repeated using an ELV viscometer. Viscosity measurement errors were measured and compared with previous results. This part of the study provides the fundamental explanations of why conventional viscometers may not accurately measure viscosities in environments that shift temperatures swiftly.

In the second part of this study, based on the above results, a novel viscometer model was designed, which was especially intended for biomedical and clinical applications. This viscometer was designed to simultaneously measure dynamic viscosity, kinematic viscosity, static viscosity, and density even when the temperatures of the test fluids increase swiftly and even when the fluid passes throughout the viscometer continuously at a speed of 1

L/min. The viscosity measurement errors were measured but could not be compared with those of conventional viscometers because none of them have such a capability.

2. Experiments

2.1. Test fluids

The viscosity and temperature characteristics of the test fluids that were used during the experiments are shown in Figure 1. The test fluids are silicone oils obtained from Shinetsu Chemical Co. These fluids are referred to as Fluid A (KF-96-100 cS), Fluid B (KF-96-1000 cS), and Fluid C (KF-96H-10,000 cS), and they present different kinematic viscosities, ν = 100, 1000, and 10,000 mm^2/s, respectively, at 25 °C, while having the same specific heat of 1.5 J/g C and the same thermal conductivity of 0.16 W/m C.

2.2. Flow visualization

As explained in detail in earlier research of this study in order to comprehend the flow movements in the experimental cup, the velocity fields were measured by particle image velocimetry (PIV) [29–32]. This confirmed to us that severe viscosity variations may occur even in very small volumes as the temperature of the fluid rises swiftly. Flow visualization in the experimental cup was achieved by introducing a small amount of nylon tracer particles into the test fluid. The diameter of the tracers for flow visualization is 20 µm and the specific gravity is 1.02. The planar measurement of the velocity field in the experimental cup was carried out using the PIV system, which consists of a CW Nd:YAG laser of 8-W power and a high-speed CMOS camera (1280 × 1024 pixels, 8 bit), which was operated by a pulse controller. The CMOS camera was located 550 mm from the test vessel. The frame rate of the camera was set to 130 frames/s and the exposure time was 7.6 ms. The focal length of the camera lens was 75 mm, with the f-number being 2.8, and the thickness of the light sheet was about 1 mm [33].

In addition to flow visualization by the PIV system, three thermocouples were also placed in different parts of the experimental cup and the heating cup. One thermocouple (T_w) was immersed into a heating cup during continuous temperature measurements. The other two thermocouples were positioned in the center (Tc) and near the wall (T_b) of the experimental cup along the long axis. Temperature measurement experiments for Fluids A, B, and C were repeated three times, and the average values were used to calculate the parameters required for the evaluation of the nonuniform temperature fields of the test fluids. During the experiments, the heater unit heated the heating water from below. The temperature readouts of all the thermocouples were recorded simultaneously. The thermocouples were located at a depth of 20 mm in the test fluid. The schematic illustration and the experimental setup for flow visualization are depicted in Figure 2.

All experiments were repeated three times to obtain statistically correct data, and three different fluids with different viscosities were used during the experiments to determine the effect of temperature on viscosity measurements. The height of the experimental cup was 40 mm and the horizontal dimensions were 64 × 24 mm. It should be mentioned that the volume of the experimental cup was 3375 cm^3 for the flow visualization experiment. Test fluids were supplied to the experimental cups up to 30 mm height in the flow visualization experiment. During the experiments, the height of the free surface of the test fluids was made equal to that of the heating cup, which was filled with water for heating the experimental cup. All experiments were initiated at room temperature (25 °C) and then the temperature was increased to 80 °C over 10 min. The PIV system could not effectively obtain any useful image because of the production of bubbles and water vapor due to boiling

after a temperature of 80 °C. Thus, the temperature increase was interrupted after 80 °C. The temperatures of the fluids were increased at a rate of 5.5 °C/min.

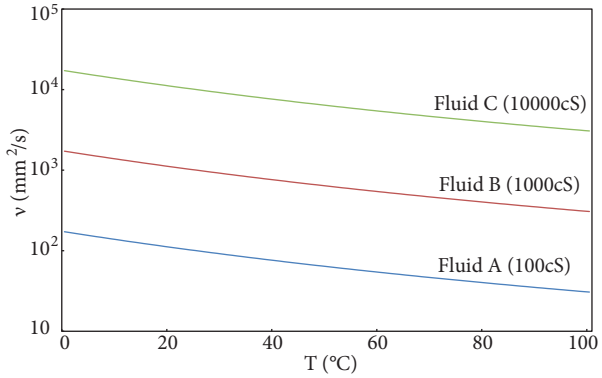


Figure 1. Kinematic viscosity temperature graphic of Fluids A, B, and C.

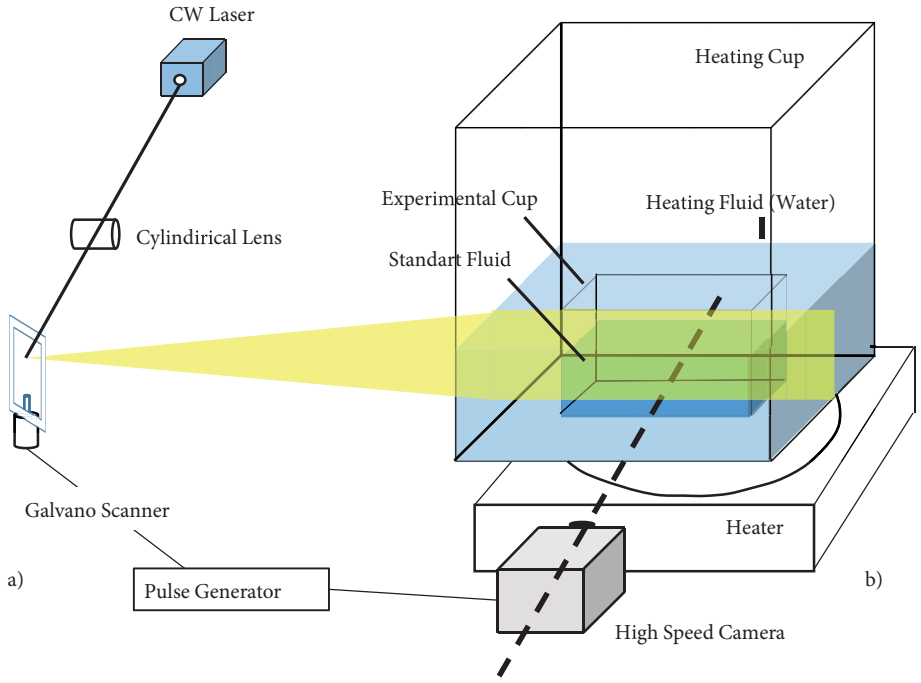


Figure 2. a) Schematic illustration of the experimental setup for flow visualization. b) Actual picture of the experimental setup for flow visualization.

2.3. ELV viscometer

As mentioned earlier, the purpose of this study was to fabricate a viscometer that can measure viscosity with a high accuracy between 0 °C and 100 °C in a time range of as much as 10 min for both Newtonian and non-Newtonian fluids from a reservoir of volume as much as 10 mL. In addition, it is expected that this viscometer can accurately measure the viscosity of fluids even when the fluids pass throughout it continuously. Furthermore, it is anticipated that this viscometer can simultaneously measure dynamic viscosity, kinetic viscosity, static viscosity, and density. None of the conventional viscometers have any of these capabilities. Therefore, the focus of this study was to develop a new type of viscometer that can achieve all of the above-mentioned goals.

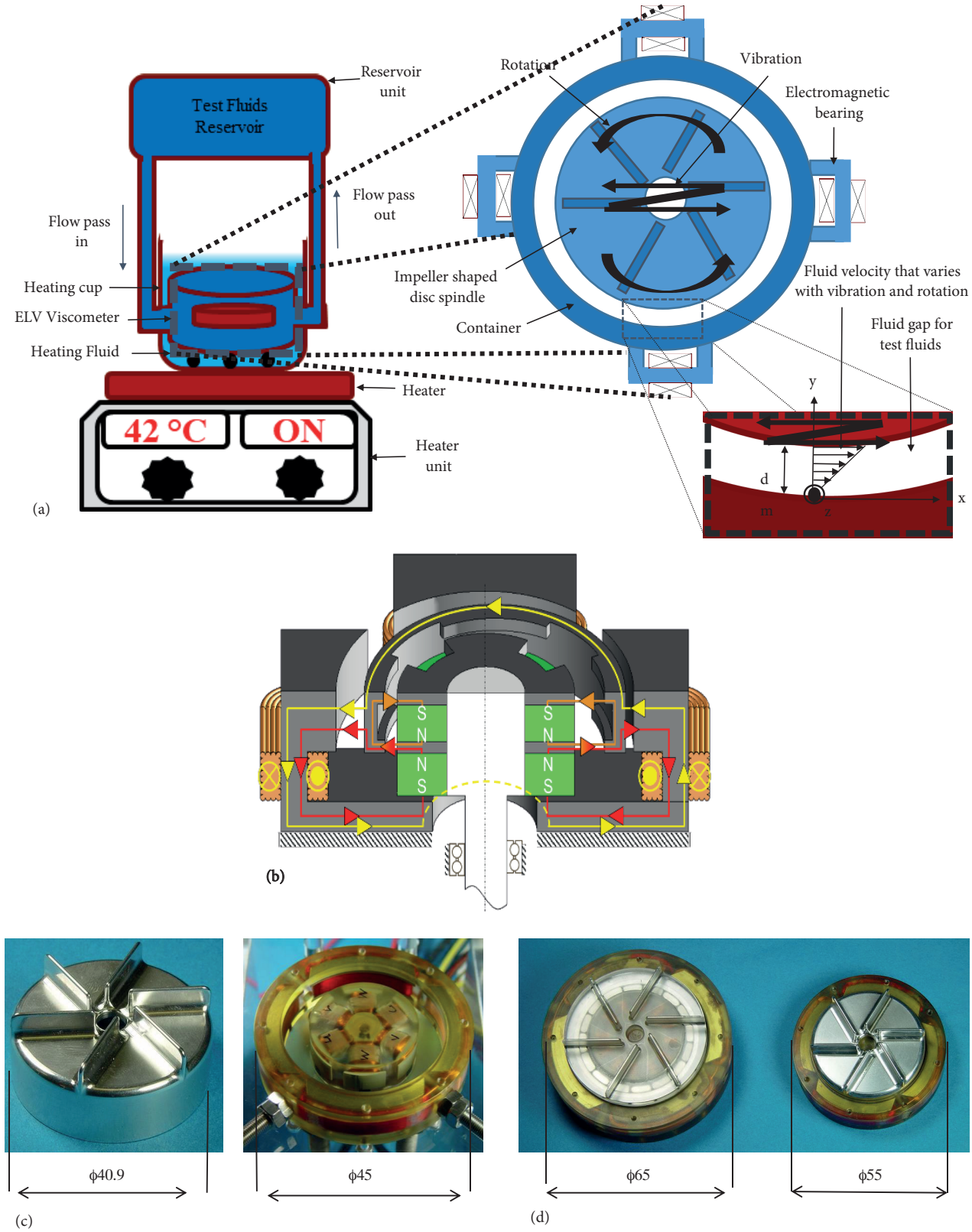


Figure 3. a) Schematic illustration of the ELV viscometer, b) schematic illustration of the conversion of the concept design of the ELV viscometer into a biomedical application, c) and d) actual pictures of the fabricated ELV viscometer ($\phi =$ mm).

Figure 3a presents the schematic illustration of the ELV viscometer that is anticipated to achieve all of the above-mentioned goals. The fundamental principle of the ELV viscometer relies on the unification of the basic concepts of a vibrational viscometer and a rotational viscometer. The mathematical background is explained in section 3. The diameter of the disc spindle is designed to be almost as large as 90% of the diameter of the container cup. This design is selected to convert turbulent flow into laminar flow. When the fluid flow is pumped into the viscometer at a high speed, there is a possibility to cause a turbulent regime along the pipelines and inside the viscometer. However, when a sizeable spindle is placed inside a container, it can obstruct the strong impacts of the turbulent regime and convert it into laminar flow unless the viscosity of the fluid is very small. Laminar flow is important because turbulent flow may affect the vibrations and rotations of the ELV viscometer and may cause inaccurate measurements.

Figure 3b presents the schematic illustration of the conversion of the concept design of the ELV viscometer into a biomedical application. This centrifugal pump may be used during cardiovascular surgery or a dialysis operation to monitor the instant viscosity changes of the blood. This design may also be utilized for biochemical or pharmaceutical engineering to monitor the instant changes of viscosity in all types of mixtures and solutions. Due to the vital importance of the problem, the ELV viscometer has been designed for biomedical applications, but it can also be easily adapted for the petroleum or beverage industries. Figures 3c and 3d present actual pictures of the fabricated ELV viscometer used as a biomedical device. The disc spindle is fabricated in an impeller shape to steer the test fluids into the desired pathways.

Figure 4a presents the schematic illustration of the ELV viscometer adapted for cardiovascular surgery. A similar structure was achieved in earlier studies of this research [34]. To fit the experiment more to real surgery conditions, the interior heater unit shown in Figure 3a is extracted. During cardiovascular surgery or dialysis, as the blood viscosity of the patient varies, it flows throughout the viscometer. Then the viscosity is measured and finally it flows back to the patient. The current design is modeled from patients undergoing cardiovascular surgery or dialysis. The test fluids are inserted into a water bath and the temperatures are increased. This causes changes in viscosities. Later, the test fluids are pumped into the ELV viscometer, the viscosity is measured, and then the fluids are pumped back to the reservoir. Temperature deviations within the mock loop are strictly measured using three different thermocouples. Flow meter and pressure sensors are used to measure the flow rate and the pressure intensity, respectively, inside the mock loop to evaluate the flow regime. If the flow regime is turbulent, the rpm of the disc spindle is decreased to convert it into laminar flow. Figures 4b, 4c, and 4d present actual pictures of the design.

3. Mathematical background

Heat distribution within a fluid can be best explained using the heat equation [35].

$$\frac{\partial T}{\partial t} - \nabla(k\nabla T) = 0 \tag{1}$$

In this equation, T denotes the temperature, t denotes the time, and k is the thermal diffusivity coefficient that is calculated as 0.07 throughout all the experiments.

This equation single-handedly proves the fact that the viscosity values will vary in every single corner of a cup as the temperature changes swiftly. Due to this reason, it will be very difficult to be certain about the exact viscosity values of a highly sensitive biochemical mixture or a small volume of a biofluid that assists clinicians about possible diseases, unless the researchers utilize water bath systems, which are expensive and not feasible at all before.

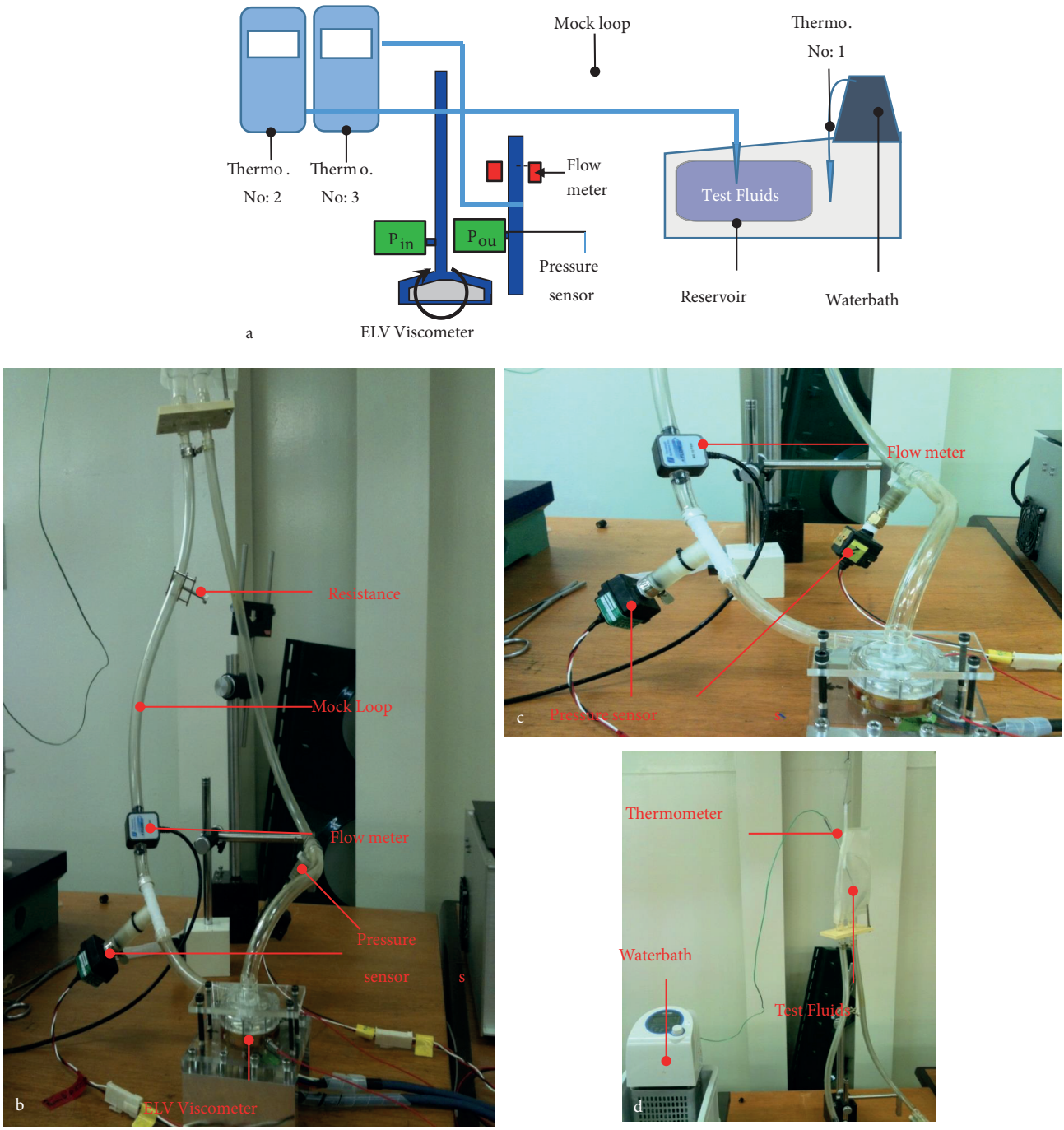


Figure 4. a) Schematic illustration of the ELV viscometer adapted for cardiovascular surgery, b), c), and d) actual pictures of the design.

For all fluids, the thermal diffusivity coefficient is 0.07 mm^2/s, the expansion coefficient is 0.00095 $(1/°C)$, and the gravitational acceleration is 9.8 m/s^2. The kinematic viscosities at different temperatures are presented in Figure 1.

On the other hand, the fundamental principle of an ELV viscometer, which is offered as a possible

solution to this problem, simply relies on the unification of a rotational viscometer and a vibrational viscometer. This helps us to obtain the dynamic viscosity, kinematic viscosity, static viscosity, and density of any fluid simultaneously. There are no viscometers across the world that can achieve this function. To understand this, the basic principles of the rotational viscometer and the vibrational viscometer should be understood first. The fundamental principle of a rotational viscometer is described below.

A rotational viscometer consists of a sample-filled cup and a measuring bob that is immersed into the test fluid. In most of the industrially available rotational viscometers, a motor drives the measuring bob and the experimental cup stands stable. The viscosity is proportional to the motor torque that is required for rotating the measuring bob against the fluid's viscous force. The principle is as follows:

$$\eta = \frac{\tau}{\gamma}, \quad \tau = \frac{M}{2\pi R_b^2.L}, \gamma = \frac{2\omega R_c^2}{R_c^2 - R_b^2} \tag{2}$$

In these equations, R_c represents the radius of the container (m), R_b is the radius of the measuring bob (m), L represents the length of the measuring bob (m), γ is the shear rate (s^{-1}), ω is the angular velocity (rad/s), τ denotes the shear stress (N/m^2), M is the measured torque (Nm), and η represents the dynamic viscosity (Pa s).

The shear rate at the surface of the bob can be calculated from the systems geometry and the angular velocity. In addition, the shear stress can be calculated from the measured torque and the geometry. Using the shear rate and shear stress, the dynamic viscosity can be obtained.

The fundamental principle of a vibrational viscometer is described below.

When a spring is oscillated under a fluid, the damping of the oscillation is related to the restorative force of the spring and the viscosity of the fluid. These parameters have a linear relationship with each other. Therefore, it should be a linear movement equation that acquires viscosity in a vibrational viscometer. In that respect, when an oscillator oscillates in an f frequency and the mechanical impedance is accepted as R_z, the linear movement equation becomes

$$_z = A\sqrt{\pi f \rho \rho}\mathbf{(3)} \tag{3}$$

In this equation, f represents the vibrational frequency (Hz), A represents the surface area of the oscillator, η represents the dynamic viscosity of the fluid, and ρ represents the fluid density. As a result, if F represents the electromagnetic force that vibrates the oscillator at a constant $\mathrm{V}e^{iwt}$ speed, then the equation is

$$R_z = \frac{F}{Ve^{iwt}} = A\sqrt{\pi f \eta \rho} \tag{4}$$

Based on this equation, the static viscosity $\eta \times \rho$ of any fluid can be determined.

As mentioned earlier, the ELV viscometer relies on unification of the principles of rotational and vibrational viscometers; therefore, the fluid density ρ can be derived when η is obtained based on the basic principle of the rotational viscometer and $\eta \times \rho$ is obtained according to the principle of the vibrational viscometer.

Finally, the kinematic viscosity ν of any fluid can be easily determined, since the formula of kinematic viscosity is

$$\nu = \frac{\eta}{\rho} \tag{5}$$

4. Results and discussion

4.1. Flow visualization

Figure 5 shows the time variation of the temperatures of test fluids in the experimental cup and that of the heating water, which were measured using the thermocouples. All the temperatures increase gradually with increasing time t after the heating starts.

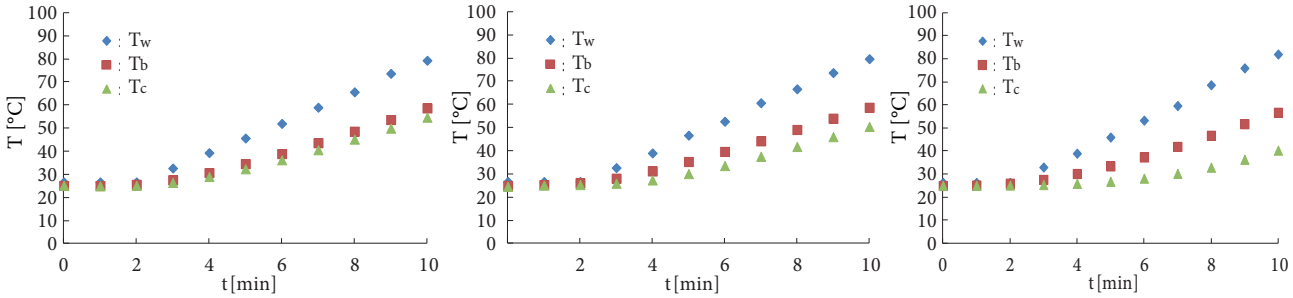


Figure 5. Time variation of nonuniform temperature fields in the flow visualization experimental cup. (a) Fluid A (100 cS); (b) Fluid B (1000 cS); (c) Fluid C (10,000 cS).

The temperatures of the test fluid and the heating water are maintained constant at the start of heating. Although the relationship between the temperature in the heating water and time is not influenced by the fluid viscosities, the temperatures Tc and Tb in the cup do change with the viscosities of the fluid and the temperature difference increases, especially for fluids with higher viscosities.

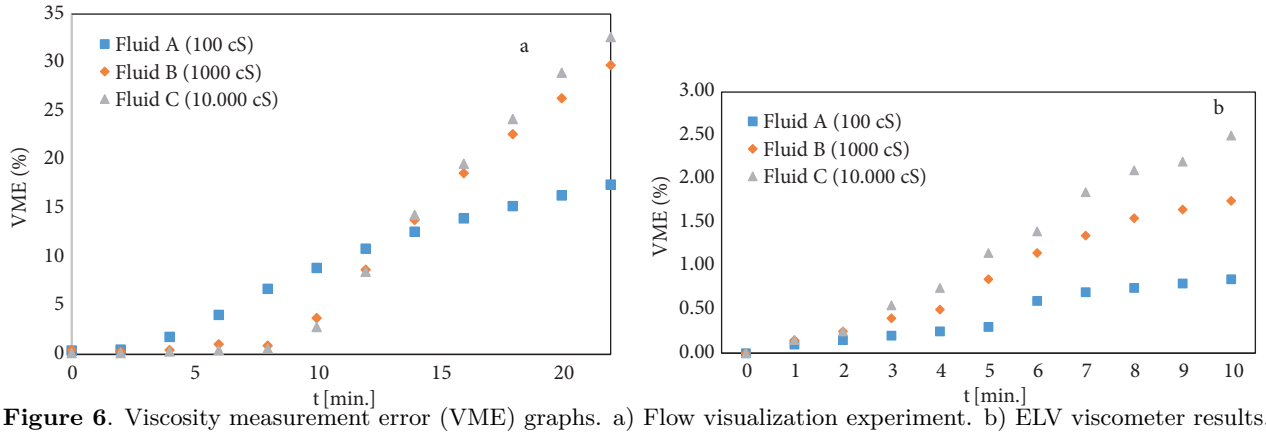


Figure 6. Viscosity measurement error (VME) graphs. a) Flow visualization experiment. b) ELV viscometer results.

As a final discussion, the VME graphic representation presented in Figure 6a describes more about the serious problems in viscosity measurement during heat transfer.

VME is calculated as follows:

$$\log\nu^t = \frac{763.1}{273+t} - 2.559 + log\nu^{25} \tag{6}$$

where ν^t : kinematic viscosity (mm^2/s) at t °C and t : −25 °C to 250 °C.

$$VME\ (\%) = \left(100 - \left(\frac{(\nu_b^t \times 100)}{\nu_c^t}\right)\right), \tag{7}$$

where ν_b^t and ν_c^t imply the viscosity of Fluids A, B, or C at the points where T_b and T_c measure the temperature (t) at selected times, respectively.

Due to high thermal convection, low-viscous fluids provide a more thermally homogenous environment, which results in lower VMEs. However, even in such advantageous conditions, 53% of VMEs occur. In high-viscous fluids, the VME results are more catastrophic. The VME increases as the heating period increases over time, resulting in almost 35% of VMEs, which makes all viscosity measurements meaningless.

4.2. ELV viscometer results

During the experiments, the disc spindle was oscillated at 75 Hz. It was anticipated that higher frequencies may cause turbulence, which can result in additional viscosity measurement errors. Furthermore, it was anticipated that lower frequencies may be difficult to detect. As a result, the oscillation frequency was optimized at 75 Hz. In addition, the fluid flow was adjusted to 1 L/min for all experiments. The use of higher flow rates was avoided as it may also cause a turbulent regime. Therefore, the disc spindle was rotated at 600 rpm for Fluid A, 800 rpm for Fluid B, and 1000 rpm for Fluid C, considering the fact that Fluid C is more viscous than Fluid A. It was observed that the change in rotation did not cause any additional VMEs. In all the experiments, the temperatures of the test fluids were increased constantly at a rate of 5.5 °C/min from 25 °C to 80 °C over 10 min.

Figure 6b presents the VME results of the ELV viscometer when there is no fluid flow throughout the viscometer. The VME results decreased substantially due to the huge disc spindle that prevents the turbulent regime and measures the viscosity inside a very small area. Using this design, the VME results decreased from 35% to 2.5%.

Figure 7a presents the dynamic viscosity results that were acquired from the ELV viscometer. The results prove that there is almost a perfect correlation (R^2) between the measured viscosity values (Fluids A, B, and C) and the real viscosity values. It appears that as much as 3% VME occurred.

Figure 7b presents the static viscosity results that were acquired from the ELV viscometer based on its vibrational principle. This is also explained in section 3. A high correlation was observed between the measured viscosity and the real viscosity values. At the maximum, 3% VME was observed.

As explained in the mathematical background of the research, the density of the fluids may be derived when the dynamic viscosity and the static viscosity of the fluids are measured. Therefore, the densities are measured as 958 kg/m^3 for Fluid A, 963 kg/m^3 for Fluid B, and 967 kg/m^3 for Fluid C, which are only 1% different from the real values of 965, 970, and 975 kg/m^3 for Fluids A, B, and C, respectively.

Figure 7c presents the kinematic viscosity results derived from the measured dynamic viscosity and the calculated density. Similar to the dynamic and static viscosity results, only 3% VME was observed in the kinematic viscosity results.

5. Conclusion

In this study, a novel design of an ELV viscometer that may have a serious impact for biomedical and clinical studies has been investigated. To achieve this, first, a swift temperature change was initiated inside an experimental cup and the flow movements were analyzed. In addition, the VMEs were calculated in such environments. Based on these results, a novel design of an ELV viscometer was constructed, which can accurately measure the viscosity from a reservoir of only 10 mL in volume and in an environment that shifts temperature swiftly from 25 °C to 100 °C within only 10 min. This viscometer has the capability to measure accurately

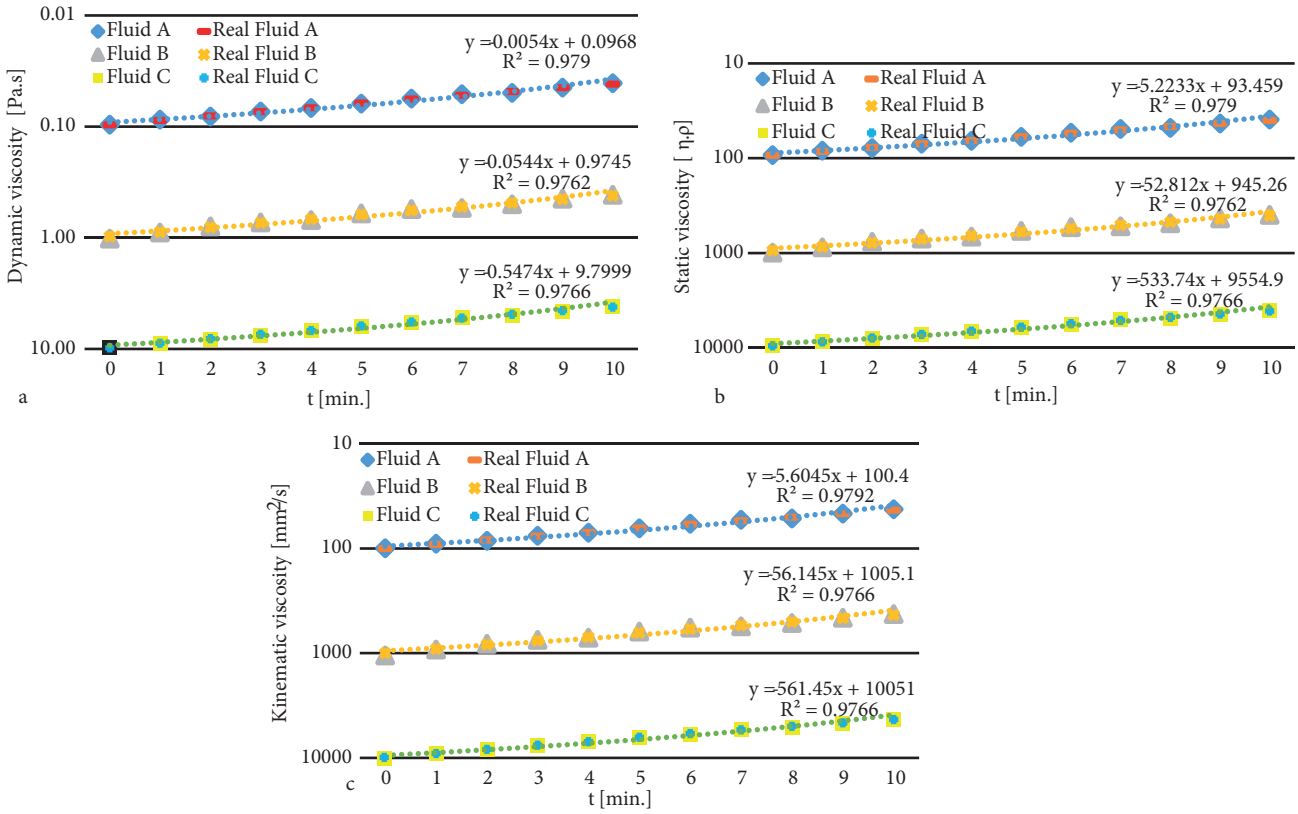


Figure 7. a) dynamic viscosity results, b) static viscosity results, c) kinematic viscosity results.

the viscosity values even when the test fluid passes throughout the experimental cup continuously. There is no viscometer in the world that can achieve this function.

Several viscometers have been developed within the last 10 years for clinical and other studies. Microfluidic viscometers that have potential to measure fluids in a range of microliters [36], viscometers for point of care applications [37], resonating viscometers that operate with sound waves [38], vibrating wire viscometers that have the potential to measure viscosities of petroleum and natural gas in deep holes [39], molecular viscometers [40] etc. have several merits for industry and academia. However, none of them have the capability to measure dynamic viscosity, kinematic viscosity, static viscosity, and density simultaneously. The proposed ELV viscometer has the capacity to obtain all these parameters for all fluids accurately in shifting temperature environments or even when the fluids are flowing through the viscometer. These characteristics make the ELV viscometer unique.

The results prove that in conventional viscometers there will be an almost 35% VME. To solve this problem, researchers have to use large water bath systems but obtain viscosity values only from a single value of temperature (primarily from 25 °C or 40 °C). This is not feasible at all and poses a serious limitation to researchers.

On the other hand, our design resulted in only a 2% VME, which is a far greater design than common viscometers. Common viscometers have no capability to accurately measure the viscosity of fluids when the test fluid passes throughout the experimental cup continuously. However, it has been proved that the ELV viscometer has the potential to achieve this almost impossible goal. Only a 2% VME was observed when the

test fluid passes throughout the vibrational viscometer at 5 L/min over 10 min as the temperature increased from 25 °C to 80 °C.

In a future study, the device may be upgraded and used at higher flow rates even for turbulent regimes. In addition, it may be validated and certificated. It is possible that this novel design of the ELV viscometer could have a serious impact for several industries such as chemical, petroleum, beverage, and pharmaceutical and, of course, for biomedical and clinical studies.

References

[1] Lowe GDO, Lee AJ, Rumley A, Price JF, Fowkes FGR. Blood viscosity and risk of cardiovascular events: the Edinburgh Artery Study. Br J Haematol 1997; 96: 168-173.

[2] Devereux RB, Drayer JI, Chien S, Pickering TG, Letcher RL, DeYoung JL, Sealey JE, Laragh JH. Whole blood viscosity as a determinant of cardiac hypertrophy in systemic hypertension. Am J Cardiol 1984; 54: 592-595.

[3] Raine AEG. Hypertension, blood viscosity, and cardiovascular morbidity in renal failure: implications of erythropoietin therapy. Lancet 1988; 331: 97-100.

[4] de Simone G, Devereux RB, Chien S, Alderman MH, Atlas SA, Laragh JH. Relation of blood viscosity to demographic and physiologic variables and to cardiovascular risk factors in apparently normal adults. Circulation 1990; 81: 107-117.

[5] Letcher RL, Chien S, Pickering TG, Sealey JE, Laragh JH. Direct relationship between blood pressure and blood viscosity in normal and hypertensive subjects: role of fibrinogen and concentration. Am J Med 1981; 70: 1195-1202.

[6] Muizelaar JP, Wei EP, Kontos HA, Becker DP. Cerebral blood flow is regulated by changes in blood pressure and in blood viscosity alike. Stroke 1986; 17: 44-48.

[7] Hunter RL, Papadea C, Gallagher CJ, Finlayson DC, Check IJ. Increased whole blood viscosity during coronary artery bypass surgery. Thromb Haemost 1990; 63: 006-012.

[8] Dormandy JA. Clinical significance of blood viscosity. Ann R Coll Surg Engl 1970; 47: 211.

[9] Yetkin F, Kayabas U, Ersoy Y, Bayindir Y, Toplu SA, Tek I. Cerebrospinal fluid viscosity: a novel diagnostic measure for acute meningitis. South Med J 2010; 103: 892-895.

[10] Chang LC, Hua CC, Liu YC, Chu CM, Chen HJ, Lee N. Pleural fluid viscosity may help identifying malignant pleural effusions. Respirology 2008; 13: 341-345.

[11] Inman BA, Etienne W, Rubin R, Owusu RA, Oliveira TR, Rodriques DB, Dewhirst MW. The impact of temperature and urinary constituents on urine viscosity and its relevance to bladder hyperthermia treatment. Int J Hypertherm 2013; 29: 206-210.

[12] Gassmann HU, Mugnier M. U.S. Patent No. 3,699,804. Washington DC, USA: U.S. Patent and Trademark Office, 1972.

[13] Tzentis LS. U.S. Patent No. 3,435,665. Washington DC, USA: U.S. Patent and Trademark Office, 1969.

[14] Bryan WL, Bryan JM. U.S. Patent No. 5,203,203. Washington DC, USA: U.S. Patent and Trademark Office, 1993.

[15] Park NA. U.S. Patent No. 5,327,778. Washington DC, USA: U.S. Patent and Trademark Office, 1994.

[16] Ball JM. U.S. Patent No. 4,750,351. Washington DC, USA: U.S. Patent and Trademark Office, 1988.

[17] Bryan WL, Bryan JM. U.S. Patent No. 5,203,203. Washington DC, USA: U.S. Patent and Trademark Office, 1993

[18] Ibar JP. U.S. Patent No. 5,885,495. Washington DC, USA: U.S. Patent and Trademark Office, 1999.

[19] Dealy JM. Challenges in process rheometry. Rheol Acta 1990; 29: 519-522.

[20] Ross RA, Kauzlarich JJ. U.S. Patent No. 5,710,374. Washington DC, USA: U.S. Patent and Trademark Office, 1998.

[21] Cohen-Tenoudji F, Ahlberg LA, Tittmann BR, Pardee WJ. U.S. Patent No. 4,779,452. Washington DC, USA: U.S. Patent and Trademark Office, 1988.

[22] Palmer AA. U.S. Patent No. 4,045,999. Washington DC, USA: U.S. Patent and Trademark Office, 1977.

[23] Boyle FP, Garvin G, Damm KW, Heath DH, George HF, Moore PJ, Robinson TE. U.S. Patent No. 6,412,338. Washington DC, USA: U.S. Patent and Trademark Office, 2002.

[24] Sakai K, Hirano T, Hosoda M. Electromagnetically spinning sphere viscometer. Appl Phys Express 2010; 3: 016602.

[25] Stabinger H, Leopold H. U.S. Patent No. 5,477,726. Washington DC, USA: U.S. Patent and Trademark Office, 1995.

[26] Plungis DW, Seymour CS, Higgins W. U.S. Patent No. 4,616,503. Washington DC, USA: U.S. Patent and Trademark Office, 1986

[27] Baek SG. U.S. Patent No. 7,290,441. Washington DC, USA: U.S. Patent and Trademark Office, 2007.

[28] Baek SG. U.S. Patent No. 7,770,436. Washington DC, USA: U.S. Patent and Trademark Office, 2007.

[29] Akpek A, Youn C, Kagawa T. A study on vibrational viscometers considering temperature distribution effect. JFPS Int J Fluid Power System 2014; 7: 1-8.

[30] Akpek A, Youn C, Maeda A, Fujisawa N, Kagawa T. Effect of thermal convection on viscosity measurement in vibrational viscometer. Journal of Flow Control, Measurement & Visualization 2014; 2: 12.

[31] Akpek A, Youn C, Kagawa T. Temperature measurement control problem of vibrational viscometers considering heat generation and heat transfer effect of oscillators. 2013 9th Asian Control Conference (ASCC), Istanbul, 2013, pp. 1-6.

[32] Akpek A. Effect of non-uniform temperature field in viscosity measurement. J Vis 2016; 19: 291-299.

[33] Kiuchi M, Fujisawa N, Tomimatsu S. Performance of PIV system for combusting flow and its application to spray combustor model. J Vis 2005; 8: 269-276.

[34] Akpek A. Development of a heart assist device as a vibrational viscometer that estimates blood viscosity. Journal of the Faculty of Engineering & Architecture of Gazi University 2018; 2018: 1-15 (article in Turkish with an abstract in English).

[35] Holman JP, Heat Transfer. 8th ed. New York, NY, USA: McGraw-Hill, 2001.

[36] Gupta S, Wang WS, Vanapalli SA. Microfluidic viscometers for shear rheology of complex fluids and biofluids. Biomicrofluidics 2016; 10: 043402.

[37] Ong PK, Lim D, Kim S. Are microfluidics-based blood viscometers ready for point-of-care applications? A review. Crit Rev Biomed Eng 2010; 38: 189-200.

[38] Heinisch M, Reichel EK, Dufour I, Jakoby B. Miniaturized resonating viscometers facilitating measurements at tunable frequencies in the low kHz-range. Procedia Eng 2011; 25: 639-642.

[39] Desroques E, Godefroy SN, Goodwin ARH, Harrison C, Hsu K, Matsumoto N. U.S. Patent No. 8,166,812. Washington DC, USA: U.S. Patent and Trademark Office, 2012.

[40] Raut SL, Kimball JD, Fudala R, Bora I, Chib R, Jaafari H, Gryczynski Z. A triazine-based BODIPY trimer as a molecular viscometer. Phys Chem Chem Phys 2016; 18: 4535-4540.